Al-Salam Journal for Engineering and Technology
Journal Homepage: http://journal.alsalam.edu.iq/index.php/ajest
e-ISSN: 2790-4822 p-ISSN: 2958-0862

Biometric Authentication Using Eyes Recognition and Shark Search Algorithm

Rasha Rokan Ismail[1]*

[1]University of Diyala , Baquba, Iraq.

*Corresponding Author: Rasha Rokan Ismail

DOI: https://doi.org/10.55145/ajest.2025.04.01.005
Received June 2024; Accepted August 2024; Available online August 2024

ABSTRACT: Iris biometrics are considered the most accurate and reliable because of their uniqueness and immutability. One of the critical difficulties that require high accuracy in the identification process and quickness in differentiating. It is preferable to reduce dimensions while keeping higher-order precision. In this paper, a technique was proposed for extracting the features of the iris image as a biometric using Shar-Smell Optimization, which works on the region of interest of the iris image is specified using the Haugh transform, the unity of features required to fix some input parameters that are selected to control the result, as well as the use of Convex Hall in determining the area that surrounds the points designated by the Haugh transform.

Keywords: Eyes Detection, Biometric Authentication, Pattern Recognition

1. INTRODUCTION

The method of identifying people using the distinctive patterns found in the iris the light-sensitive layer located at the back of the eye is known as iris biometrics [1]. Security processes in biometric authentication systems are based on the uniqueness of the biological traits of individuals. These systems work on comparing the biometric data capture to store it in a database. The eyes and their iris are considered biometrics that offer several opportunities for identification [2]. The main advantages of iris recognition are iris stability and protectability since it is inside the eye, additionally, it is fast for matching and has resistance to false matching. To find the efficient pattern a sequence of processing is required and may need an optimization algorithm. The algorithms of optimization minimize or maximize several fitness functions relating to several sets, generally, they represent a range of selections insisting on a specific condition. The fitness function provides a comparison among various selections to determine which one is the best [3]. Therefore, to achieve this goal, recently, different meta-heuristic optimization algorithms were suggested in the literature like a genetic algorithm (GA) [4], particle swarm optimization (PSO) [5], ant colony optimization (ACO) [6], Artificial bee colony (ABC), honey bee mating optimization (HBMO) [7], Bacterial Foraging (BF) [8], Invasive Weed Optimization (IWO) [9], Clonal Selection Algorithm (CSA) [10], Evolutionary Algorithm (EA) [11], Shuffled Frog Leaping Algorithm (SFLA) [12].

Using the iris image to identify people is an important matter, and the process of strengthening this method, improving it, and reducing the time required is an important matter in this paper. Shark Smell Optimization was employed to identify important areas in the eye image to be used in identifying people instead of using a complete image. The rest of the paper contains related work, an explanation of Shark Smell Optimization, a proposed method, experimental test results, and a conclusion.

2. RELATED WORKS

• Two different intrusion detection (ID) categorization systems, each with unique use cases, were presented by Ogundokun, Roseline Oluwaseun, et al. [13]. The Particle Swarm Optimization (PSO) approach was used to minimize the dimensionality prior to using the two classifiers for the classification procedure. The techniques for categorizing abnormalities in networks were examined. The two classifiers that are employed are PSO + Decision Tree (PSO+DT) and PSO + K-Nearest Neighbor (PSO+KNN). The results of the detection algorithms were verified using the KDD-CUP 99 dataset.

*Corresponding author: Rasha.roka.ismail@gmail.com

• The model proposed by Almomani, Omar [14] used wrapper-based methods in conjunction with the GA, PSO, GWO, and FFA algorithms for feature selection, and filtering-based methods for the mutual information (MI) of the GA, PSO, GWO, and FFA algorithms, which generated 13 sets of rules. The J48 ML classifier, the support vector machine (SVM), and the UNSW-NB15 dataset are used to assess the features derived from the proposed model.

•Rostami et al. [15] proposed a three-step process for feature selection based on a genetic algorithm based on community detection: first, feature similarities are computed; second, community detection techniques classify the attributes into clusters; and third, a genetic algorithm selects features utilizing a novel community-based repair process. The approach looked at the efficacy of the suggested solution in nine benchmark categorization problems. Additionally, the authors have compared the efficacy of the recommended approach with the outcomes of four distinct feature selection algorithms.

3. SHARK SMELL OPTIMIZATION (SSO)

The depth-first search approach, which is based on the shark's remarkable sense of smell, is implemented using the meta-heuristic algorithm SSO. The construction of mathematical formalization is based on a number of assumptions that underpin the SSO approach. Among these theories is [16]: blood is injected into the water (searching space) when the fish is injured. Because blood injection into seawater happens often, the injfish's fish velocity may be disregarded in favor of the shark's movement velocity [17]. The following stages provide a concise overview of this procedure:

Initializing

The procedure of searching is started when the shark detects the odor of the injured prey particle. The population of the initial solution represents the shark locations. The vector of the start location is given as follows [18]:

$$X_i = [X_1^1, X_2^1, \dots\dots, X_{NP}^1] \text{ and NP = Population Size} \quad \dots (1)$$

Where X_i Denotes i^{th} beginning position vector (i^{th} initial candidate solution), the speed of every individual of the population is presented by:

$$SP_i = [SP_{i,1}^1, SP_{i,2}^1, \dots\dots, SP_{i,ND}^1] \quad \text{,i=1..., NP} \quad \dots. (2)$$

Where is jth dimension of the ith shark location or jth decision variable of the ith location of the shark , and ND denotes the number of decision variables in the problem of optimization [19]. Nevertheless, the fitness function of the pertinent individual can be identified via OF (XNP) and will be kept to every individual after iteration. It is assumed that the algorithm is initiated at the zero iteration [20].

3.1 SHARK MOVEMENT TOWARD THE PREY

The sharks moving to seek prey is the next stage of initialization. The shark moves in two directions: forward and backward. The shark moves in the direction of its prey by using the following formula to determine its odor [21]:

$$SP_{i,j}^m = \mu_m . R1. \frac{\vartheta(OF)}{\vartheta X_j} \left[X_{i,j}^m + \alpha m. R2. SP_{i,j}^{m-1}\right] \quad \dots (3)$$

Where i = 1, ⋯, NP, j = 1, ⋯,ND, m = 1, ⋯, M, ∇(OF) represents the fitness function gradient, $\boldsymbol{\mu_m}$ is the gradient coefficient, M represents the maximum number of stages in the forward shark movement and belongs to the interval (0, 1], R1 and R2 indicate the constants that are randomly generated, and m is the number of the stages [22]. There is a restriction to the speed of shark that is given as follows:

$$\left|SP_{i,j}^m\right| = \left[\mu_m . R1. \frac{\vartheta(OF)}{\vartheta X_j} \left|X_{i,j}^m + \alpha m. r2. SP_{i,j}^{m-1}, \left|\gamma_m . SP_{i,j}^{m-1}\right|\right|\right] \quad \dots (4)$$

Where i = 1, ⋯, NP, j = 1, ⋯, ND, m = 1, ⋯, M, γ_m The parameter indicates the maximum boundary of the current speed regarding the preceding speed. Every constituent $SP_{i,j}^m$ of the SP_i^m Is computed in the above Equation. For the shark universal seeking, the updated location assessment can be obtained as follows:

$$GY_i^{m+1} = X_i^m + SP_i^m . \Delta tm \quad \dots (5)$$

The interval of time to m^{th} stage is identified by Δtm. Therefore, the shark's local seeking can be given by:

$$NX_i^{m+1,l} = GY_i^{m+1} + R3. \Delta GY_i^{m+1} \quad \dots (6)$$

Where l = 1, ⋯, L, R3 denotes a constant that is generated haphazardly in the interval (−1, +1); and L denotes the number of the points in the local seek of every stage. The optimal point that is searched in the local search and forward movement are selected via the shark and modeled in the shark smell optimization algorithm as follows:

$$X_i^{K+1} = \text{orgmax}\left\{OF(GY_i^{m+1}), OF\left(NX_i^{m+1,1}\right), .., OF\left(NX_i^{m+1,L}\right)\right\} \quad \dots (7)$$

i =1, 2, ..., NP.

4. HOUGH TRANSFORMATION FOR CIRCLE DETECTION

These days, one of the most used techniques for finding circles is the Hough transform approach. More time and storage space are needed in the parameter space since the classic Hough transform technique requires three-dimensional voting to the radius, center, and circle parameters. The conventional Hough transform approach's basic tenet is outlined below [22]. Here is the circle equation:

$$(x-a)^2 + (y-b)^2 = r^2 \quad \ldots (8)$$

where r denotes the radius and (a, b) the circle's center.

While the (a, b) parameter and r shift to an unknown number, the detected (x, y) coordinates show the amount within the parameter space. Therefore, each feature point (x, y) may form a cone in the a-b-r parameter space. Each cone in the picture space representing a feature point on a circle should come together at a single point. Finding this point indicates that, as shown in Figure (1), the coordinates of (a, b, r) represent the circular center and radius.

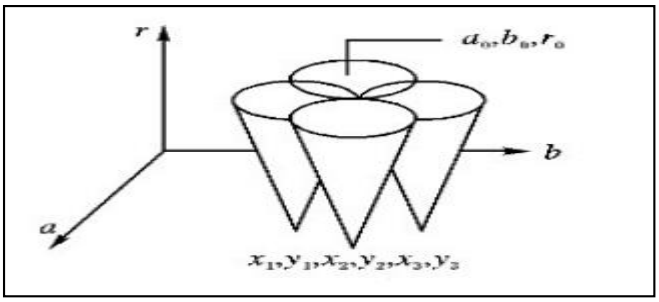

FIGURE 1. - Circle within parameter space [19]

5. CONVEX HULL ALGORITHM

A very small portion of the set of points are the vertices of the convex hull. Most of the points are located on the convex hull. Take away as many spots from outside the convex hull as you can. Convex hulls are often used in several fields, Shape Matching being one of them [23]. Computational geometry states that an object is convex in Euclidean space if every point on the straight-line segment connecting every pair of points within the object is also inside the object.

6. NORMALIZATION OF IRIS IMAGE

The frequency and spatial domains influence the iris image normalizing techniques. Author T. Spencer created a shade correction technique inside the space approach in [24], which involves subtracting the backdrop picture from the original fund's photos. To estimate the backdrop picture, a large-sized median filter might be used. The author Niemeijer has used this technique with color iris photos in [25]. Furthermore, the authors of [26] described how to use enhanced statistical techniques for the histogram to normalize and increase contrast.

7. PROBABLISTIC NEURAL NETWORK (PNN)

PPN typically consists of four layers: output, competition, hidden, and input. The input layer first provides the network with the feature vector and a number of sample features. Secondly, the connection weight connects the hidden layer to the input layer. It computes the similarity between the feature input vector and every mode in the training set, then feeds that distance into the Gaussian function to produce the output of the hidden layer [27]. In this instance, the number of neurons indicates the number of input sample vectors. Third, each class's pattern layer units are joined by the competition layer. The quantity of sample categories is indicated by the number of neurons in this layer. The output layer finally provides the highest score that may be obtained.

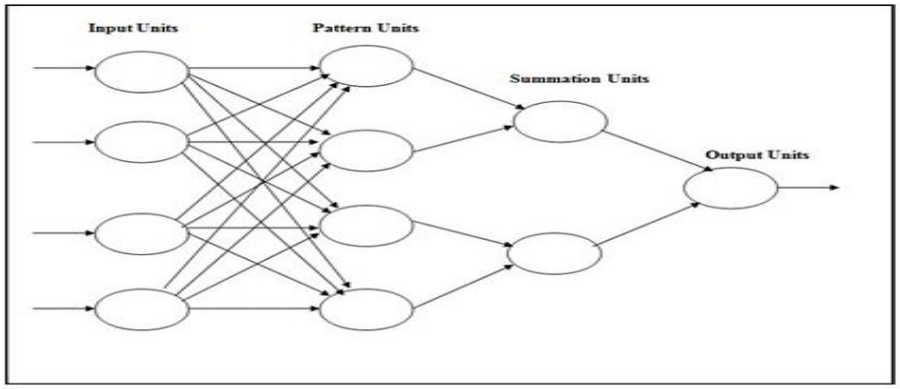

FIGURE 2. - Architecture of Probability Neural Network [28]

8. PROPOSED METHOD

To increase the accuracy of identification, iris pictures must be used as a biometric during authentication. Light may initially be seen striking the iris via the pupil of the eye, a black hole in the middle of the iris. Light beams entering the pupil are either immediately absorbed by the tissues within the eye or absorbed after diffuse reflections inside the eye, which often miss leaving the small pupil, which is why it seems dark. The human pupil is spherical, despite variations in shape. between species. The iris is the aperture stop and the anatomical pupil is the eye's aperture, according to optical terminology.

The entry pupil, which is magnified by the cornea and appears as an image from the outside of the eye, does not precisely match the real pupil's size and location. The embryonic pupil's covering, the embryonic pupillary membrane, confluences at the collarette, a prominent structure on the inner border. The first step in the localization process is to identify the eye region in the input image by using the Haugh transform for circle identification, which finds the pupil. This area, as shown in the picture, is regarded as a Region of interest (ROI) that was clipped in order to be handled in step (4).

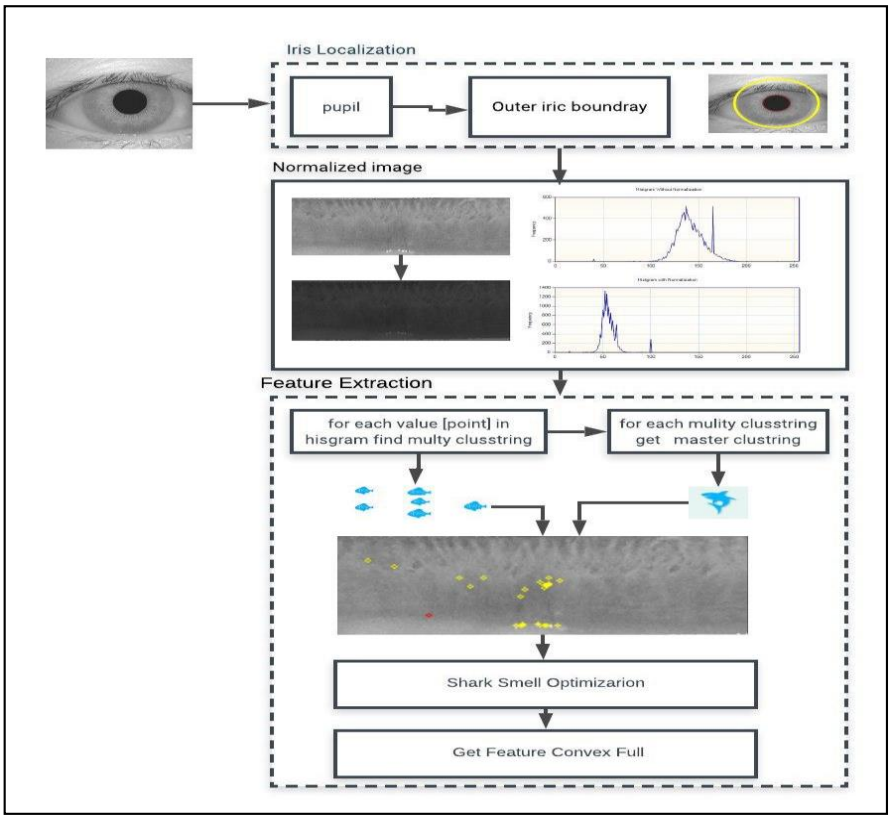

FIGURE 3. - Proposed method framework

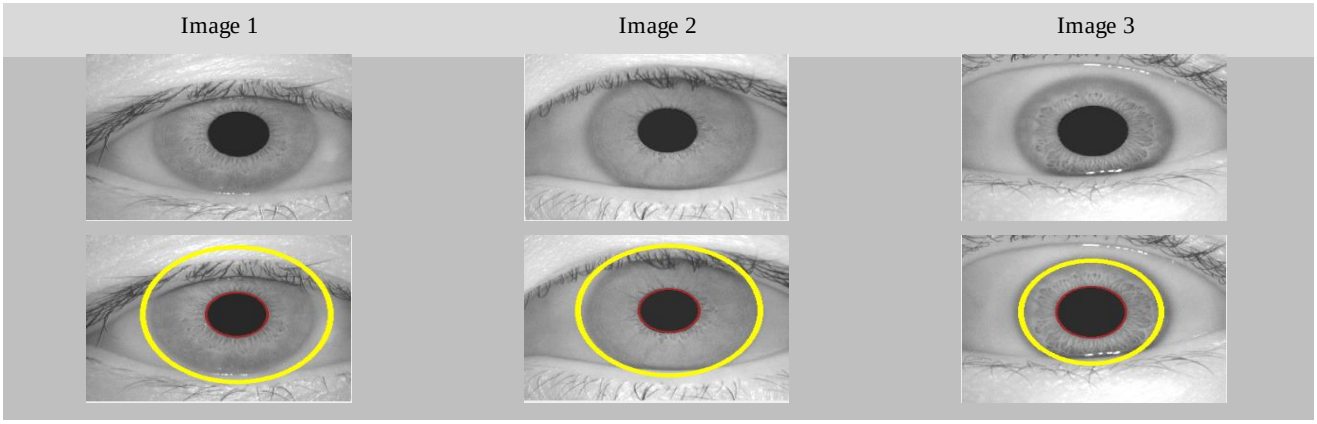

FIGURE 4. - ROI detection using Haugh transform

The ROI is normalized by transferring it into a rectangle region by applying a certain amount of radius that will represent the rectangular region with interpolation of each point that does not depend on the radius, as shown in Figure (5). The normalization is represented by transforming the values of the given area of the region in which the shark algorithm is executed to determine the best section of the region for extracting features.

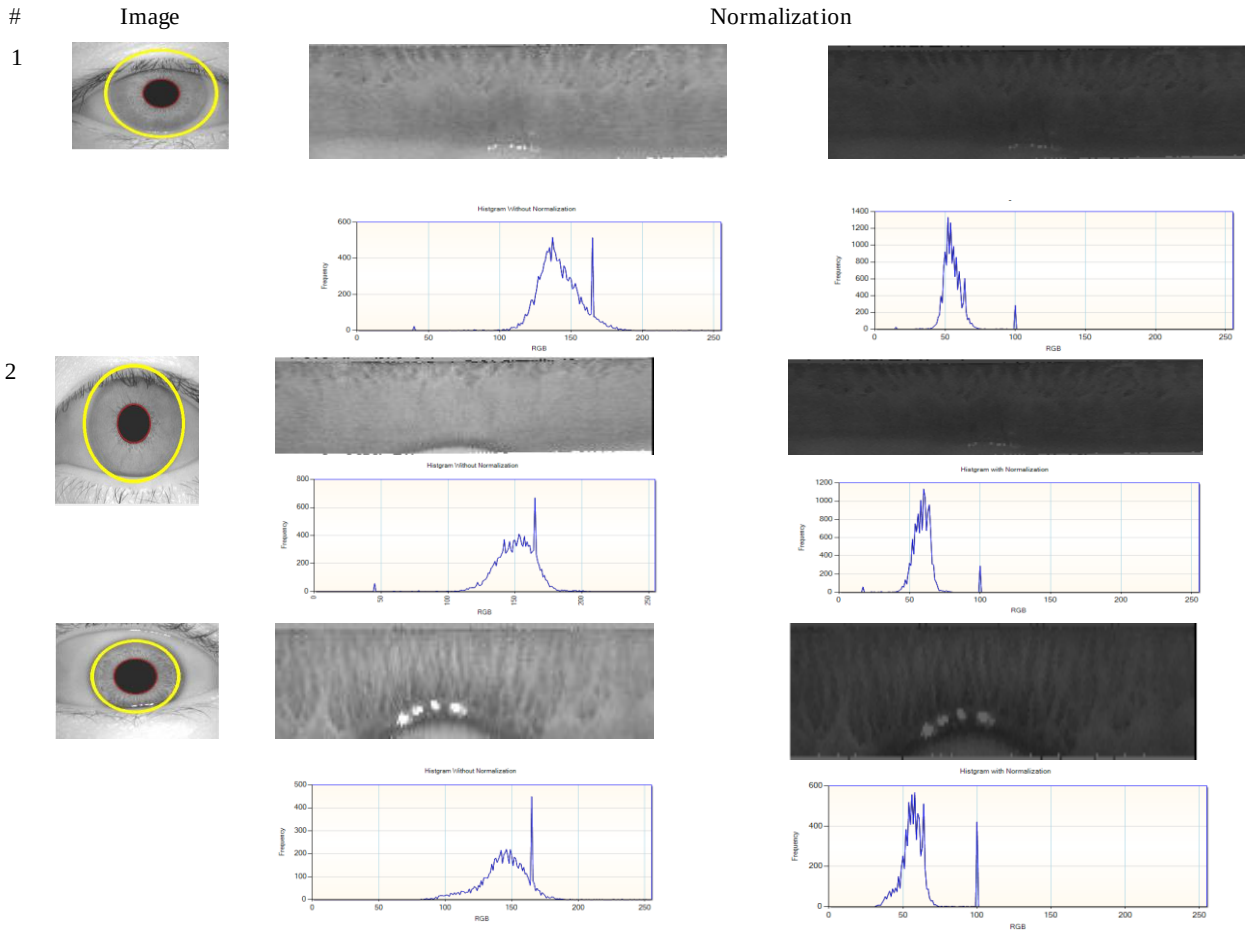

FIGURE 5. - Normalization of ROI

Several beginning points are used to specify the initial populations. Each value in the histogram is treated as a cluster, and the points are obtained if they are larger than a particular threshold (considered as parameters). Each cluster is processed, and its center is employed as a fish. The number of points (fish) in which the center is assumed to be a shark (the starting point). The process of starting and attaining the objective is depicted in Figure (6), tracking two things, the first is termed forward process that depends on neighbor search mask for example (3×3), (5×5) or (7×7).

Each job point is evaluated about two different fish and the best one is chosen. The second factor is the rotation in place (or lack thereof), which determines when a new location is established.

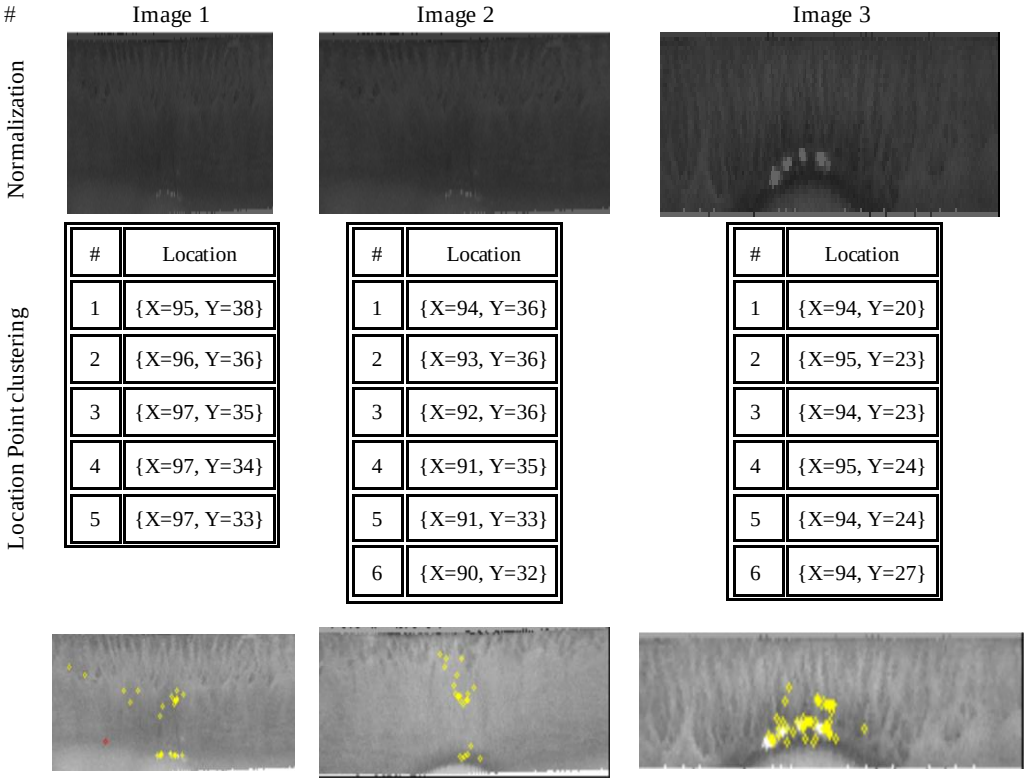

#	Location
1	{X=95, Y=38}
2	{X=96, Y=36}
3	{X=97, Y=35}
4	{X=97, Y=34}
5	{X=97, Y=33}

#	Location
1	{X=94, Y=36}
2	{X=93, Y=36}
3	{X=92, Y=36}
4	{X=91, Y=35}
5	{X=91, Y=33}
6	{X=90, Y=32}

#	Location
1	{X=94, Y=20}
2	{X=95, Y=23}
3	{X=94, Y=23}
4	{X=95, Y=24}
5	{X=94, Y=24}
6	{X=94, Y=27}

FIGURE 6. - Initial population specification

9. RESULTS AND DISCUSION

The proposed method applied to images got it from the CASIA-IrisV3 dataset provides a thorough compilation for iris recognition studies. It contains 22,035 near-infrared iris pictures in grayscale from more than 700 people. This dataset's diversity and high image quality make it useful for creating and testing iris recognition systems. The proposed approach is being evaluated to determine its applicability. As indicated in the graphic, shark behavior is determined by a collection of random variables that represent the diversity of optimization solutions in Figures (7). The shark's direction is determined by the relationship between the existing points in the neighbor mask and all of the fish in state space. The SSO implementation creates a path from the beginning point (shark) to the fish, and this path varies depending on the parameters, as illustrated in Figures (8) and Figures (9).

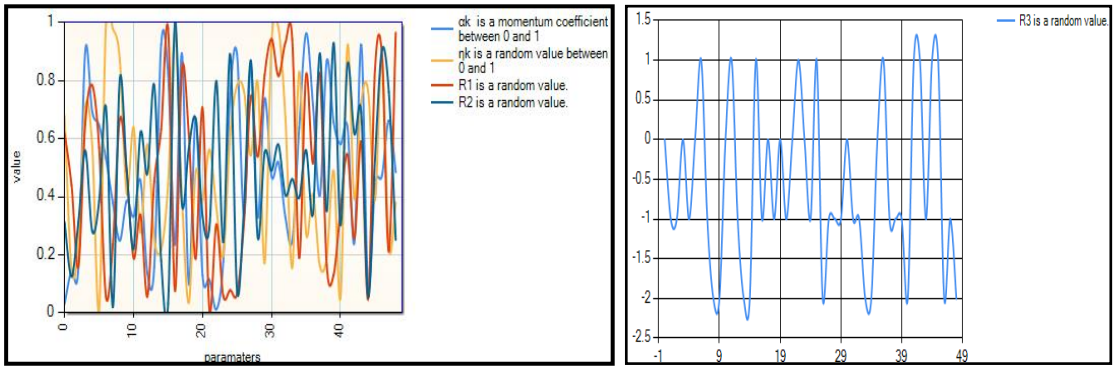

FIGURE 7. - Random Variable in SSO

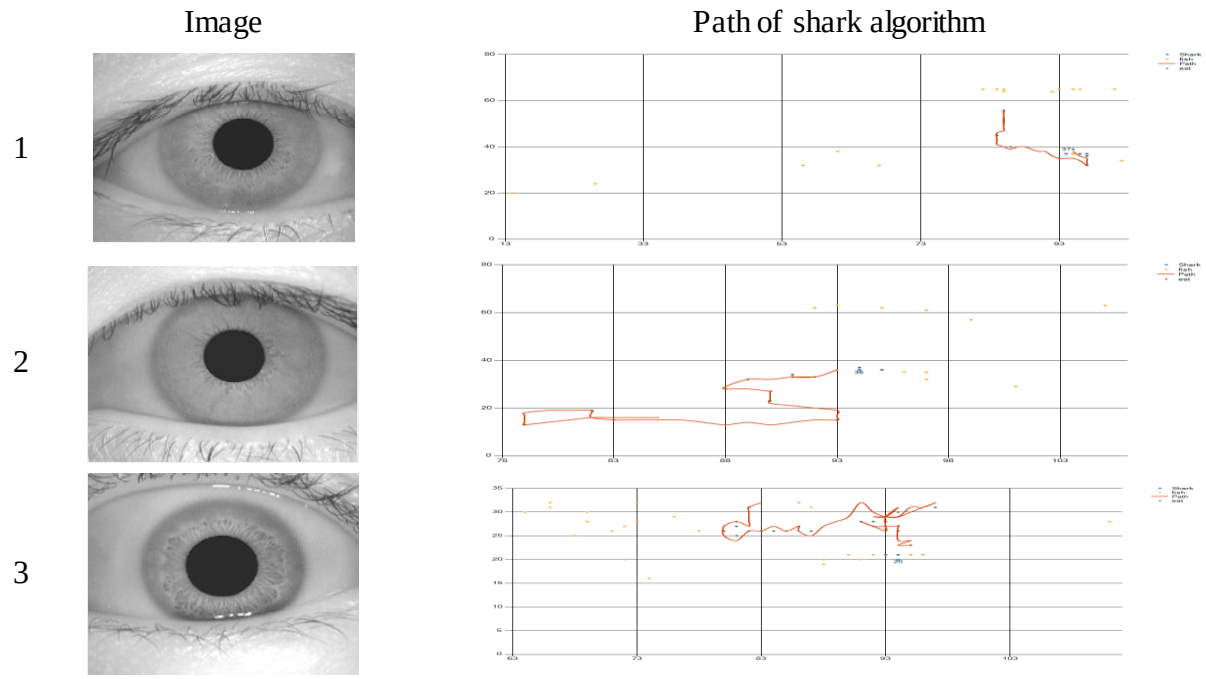

FIGURE 8. - The path produced by a shark

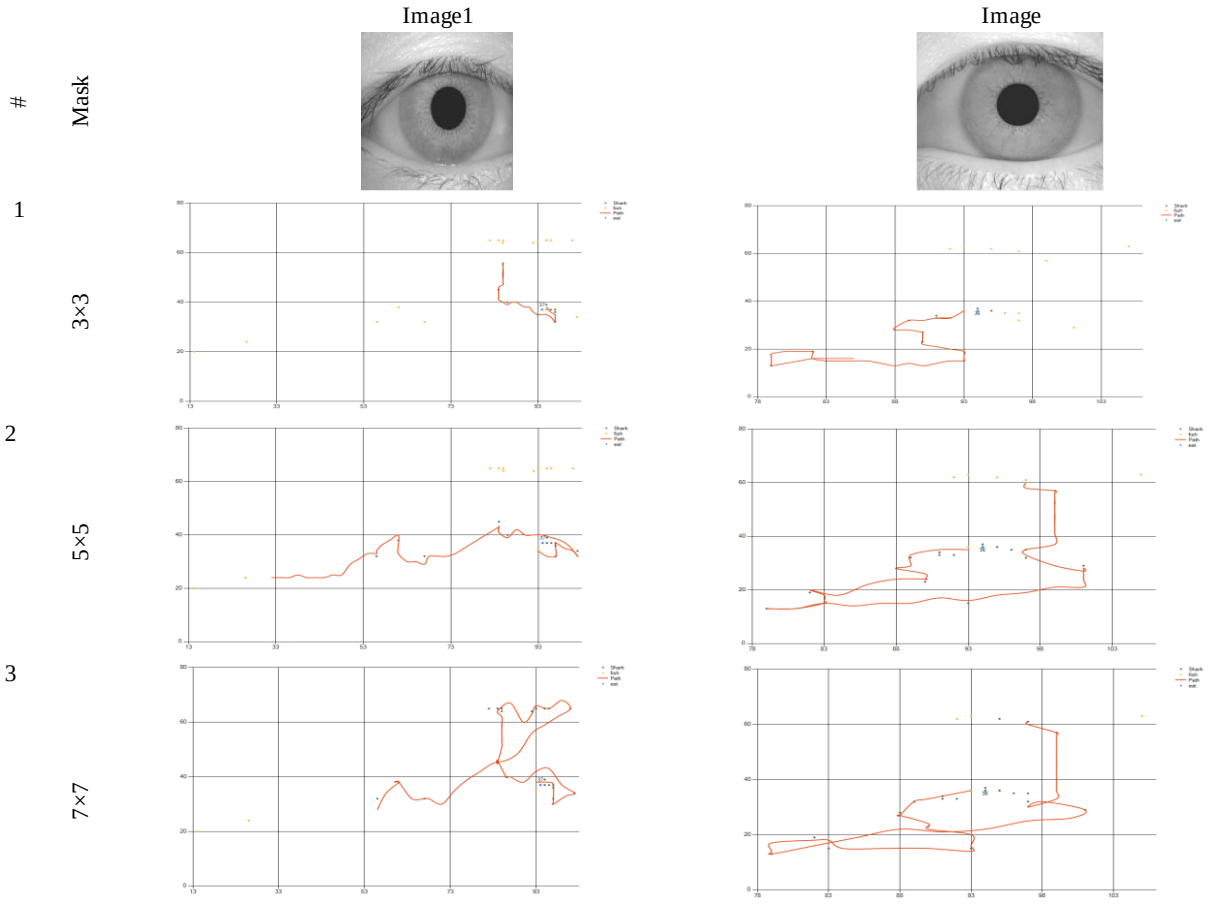

FIGURE 9. - Different paths in different masks

After SSO has stopped and found the way, the points are taken by Convex Hall, which produces an area whose attributes are unique fromone user to the next. This attribute is picture feature extraction, as seen in Figure (10).

The extracted features tested are explained in table (1) of two images for different masks (3×3), (5×5) and (7×7). These features are statistical [29] and will be normalized and used for classification.

Table 1. - Feature extraction examples

#	Feature	Image 1			Image 2		
		3*3	5*5	7*7	3*3	5*5	7*7
1	Rec Area	4761	203.6	3426.43	324	0.101	484.4
2	Rec Perimeter	77.85	16.102	66.05	20.31	0.35	24.83
3	Mean	27.058	8.485	25.025	9.9858	12.1971	23.76
4	Variance	108.92	6.577	47.61	20.63	58.75	59.98
5	Std	10.436	2.564	6.900	4.542500	7.665	7.745
6	Skewness	0.0374	0.13395	-0.0008	-9. E-08	0.1138	-0.003
7	Kurtosis	0.0627	0.2364	0.00024	1.E-09	0.304	0.0015
8	Equivalent Diameter	77.8581	16.1028	66.0505	20.31082	0.3597	24.831
9	Solidity	466.5	119.5	595.5	67.5	216.5	207.5

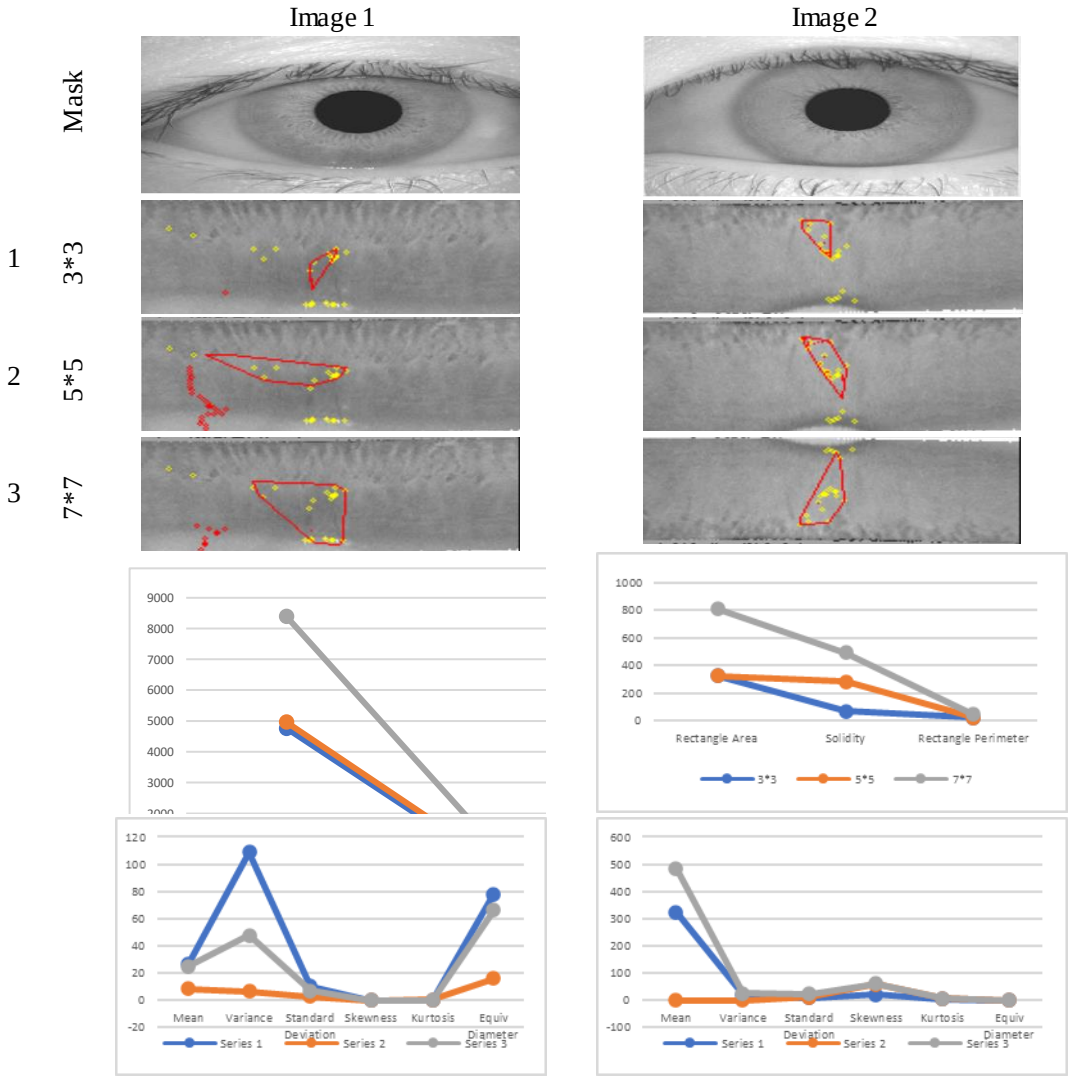

FIGURE 10. - properties of feature extraction

The retrieved features were evaluated on the Casia data set using a probabilistic neural network for version 1, version 2, and version 3. (PNN). The classification accuracy was high, as shown in Table 2, and the comparison of these data is displayed in Figure (11).

Table 2. - Feature extraction examples

#	Parameter PNN	Type dataset		
	Semi	Casia V1.0	Casia V2.0	Casia V3.0
1	0.011	98.146	96.537	96.20
2	0.223	99.674	99.748	97.92
3	0.345	98.757	97.728	91.428

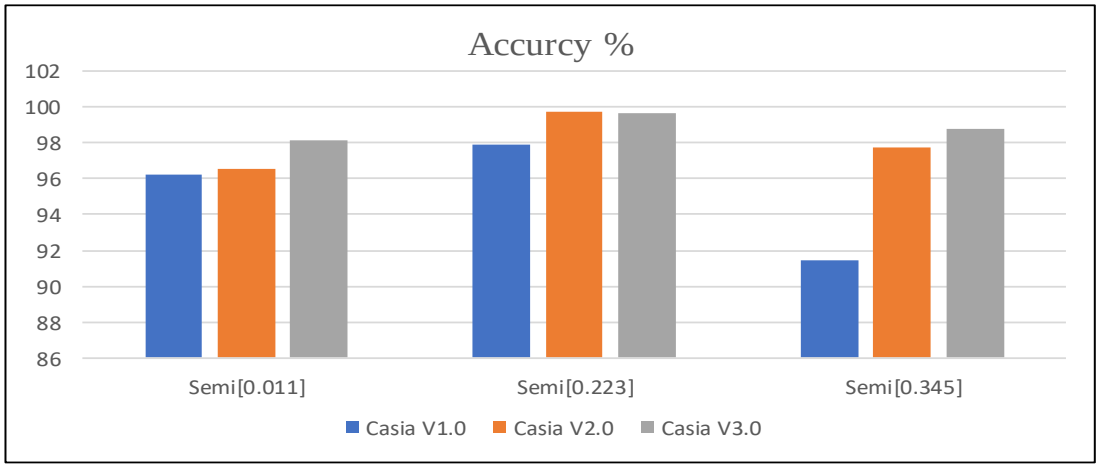

FIGURE 11. - the comparison of accuracies of Casia versions

10. Conclusion

Due to their immutability and uniqueness, iris biometrics are thought to be the most accurate and dependable one of the crucial challenges that call for rapid differentiation and excellent identification accuracy. Reducing dimensions without sacrificing higher-order precision is desirable. In this paper, a method for extracting the features of an iris image as a biometric was proposed using Shar-Smell Optimization. The technique relies on the Haugh transform to specify the region of interest of the iris image, the unity of features needed to fix some input parameters chosen to control the result, and Convex Hall to determine the area surrounding the points designated by the Haugh transform. The route of the shark is used in collecting fish, which are the methods used in the application of the Convex Hull Algorithm, and the outcomes of this algorithm rely on the mask used.

FUNDING

None

ACKNOWLEDGEMENT

The authors would like to thank the anonymous reviewers for their efforts.

CONFLICTS OF INTEREST

The authors declare no conflict of interest

REFERENCES

[1] L. Semerád and M. Drahanský, "Retina recognition using crossings and bifurcations," in Applications of Pattern Recognition, IntechOpen, 2021.

[2] N. Liu and R. Yao, "The Crawling Strategy of Shark-Search Algorithm Based on Multi Granularity," in 2015 8th International Symposium on Computational Intelligence and Design (ISCID), 2015, doi: 10.1109/iscid.2015.273.

[3] L. Qiu, Y. Lou, and M. Chang, "Research on theme crawler based on Shark-Search and PageRank algorithm," in 2016 4th International Conference on Cloud Computing and Intelligence Systems (CCIS), 2016, doi: 10.1109/ccis.2016.7790267.

[4] O. Abedinia, N. Amjady, and A. Ghasemi, "A new metaheuristic algorithm based on shark smell optimization," Complexity, vol. 21, no. 5, pp. 97–116, 2016.

[5] S. Mohammad-Azari, O. Bozorg-Haddad, and X. Chu, "Shark Smell Optimization (SSO) Algorithm," Studies in Computational Intelligence, pp. 93–103, 2017, doi: 10.1007/978-981-10-5221-7_10.

[6] M. Bagheri, A. Sultanbek, O. Abedinia, M. S. Naderi, and N. Ghadimi, "Multi-objective Shark Smell Optimization for Solving the Reactive Power Dispatch Problem," in 2018 IEEE International Conference on Environment and Electrical Engineering and 2018 IEEE Industrial and Commercial Power Systems Europe (EEEIC / I&CPS Europe), 2018, doi: 10.1109/etc.2018.8494502.

[7] Y. Rao, Z. Shao, A. H. Ahangarnejad, E. Gholamalizadeh, and B. Sobhani, "A Shark Smell Optimizer applied to identify the optimal parameters of the proton exchange membrane fuel cell model," Energy Conversion and Management, vol. 182, pp. 1–8, 2019, doi: 10.1016/j.enconman.2018.12.057.

[8] D. Matrokhin and R. Golovanov, "Convex hull calculation approach based on BST," in 2018 IEEE Conference of Russian Young Researchers in Electrical and Electronic Engineering (EIConRus), 2018, doi: 10.1109/eiconrus.2018.8317394.

[9] F. Preparata and S. Hong, "Convex hulls of finite sets of points in two and three dimensions," Communications of the ACM, vol. 20, no. 2, pp. 87-93, 1977.

[10] R. Graham, "An efficient algorithm for determining the convex hull of a finite planar set," Information Processing Letters, vol. 1, no. 4, pp. 132-133, 1972.

[11] F. Preparata, "An optimal real-time algorithm for planar convex hulls," Communications of the ACM, vol. 22, no. 7, pp. 402-405, 1979.

[12] C. Barber, D. Dobkin, and H. Huhdanpaa, "The quickhull algorithm for convex hulls," ACM Transactions on Mathematical Software, vol. 22, no. 4, pp. 469-483, 1996.

[13] D. Kirkpatrick and R. Seidel, "The Ultimate Planar Convex Hull Algorithm?" SIAM Journal on Computing, vol. 15, no. 1, pp. 287-299, 1986.

[14] R. O. Ogundokun et al., "An enhanced intrusion detection system using particle swarm optimization feature extraction technique," Procedia Computer Science, vol. 193, pp. 504-512, 2021.

[15] O. Almomani, "A feature selection model for network intrusion detection system based on PSO, GWO, FFA and GA algorithms," Symmetry, vol. 12, no. 6, p. 1046, 2020.

[16] M. Rostami, K. Berahmand, and S. Forouzandeh, "A novel community detection based genetic algorithm for feature selection," Journal of Big Data, vol. 8, no. 1, p. 2, 2021.

[17] T. Chan, "Optimal output-sensitive convex hull algorithms in two and three dimensions," Discrete & Computational Geometry, vol. 16, no. 4, pp. 361-368, 1996.

[18] L. Huang and G. Liu, "Proved quick convex hull algorithm for scattered points," in 2012 International Conference on Computer Science and Information Processing (CSIP), 2012, doi: 10.1109/csip.2012.6309116.

[19] H. R. Khosravani, A. E. Ruano, and P. M. Ferreira, "A simple algorithm for convex hull determination in high dimensions," in 2013 IEEE 8th International Symposium on Intelligent Signal Processing, 2013, doi: 10.1109/wisp.2013.6657492.

[20] P. Subbuthai and S. Muruganand, "Restoration of retina images using extended median filter algorithm," in 2015 2nd International Conference on Signal Processing and Integrated Networks (SPIN), 2015, doi: 10.1109/spin.2015.7095378.

[21] Y. Yi and D. Zhang, "Observation model-based retinal fundus image normalization and enhancement," in 2011 4th International Congress on Image and Signal Processing, 2011, doi: 10.1109/cisp.2011.6100324.

[22] T. Spencer, J. A. Olson, K. C. McHardy, P. F. Sharp, and J. V. Forrester, "An image-processing strategy for the segmentation and quantification in fluorescein angiograms of the ocular fundus," Comput. Biomed. Res., vol. 29, pp. 284–302, 1996.

[23] M. Niemeijer, B. van Ginneken, J. Staal, M. S. A. Suttorp-Schulten, and M. D. Abràmoff, "Automatic detection of red lesions in digital color fundus photographs," IEEE Trans. Med. Imag., vol. 24, no. 5, pp. 584–592, 2005.

[24] T. S. Lin, M. H. Du, and J. T. Xu, "The Preprocessing of subtraction and the enhancement for biomedical image of retinal blood vessels," J. Biomed. Eng., vol. 20, no. 1, pp. 56-59, 2003.

[25] J. B. Zimmerman and S. M. Pizer, "An evaluation of the effectiveness of adaptive histogram equalization for contrast enhancement," IEEE Trans Med. Imaging, vol. 7, no. 4, pp. 304-312, 1988.

[26] S. Intajag, P. Wattanayingcharoen, and V. Tipsuwanpom, "Retinal image enhancement by multi histogram equalization," in Proceedings Joint International Conference on Information Communication Technology: JICT2007, Vientiane, Lao PDR, 2007, pp. 101-105.

[27] X. Wang, L. Dong, S. Liu, Y. Hao, and B. Wang, "A Fault Classification Method of Photovoltaic Array Based on Probabilistic Neural Network," in 2019 Chinese Control and Decision Conference (CCDC), 2019, doi: 10.1109/ccdc.2019.8832338.

[28] P. V. C. Hough, "Method and means for recognizing complex patterns," U.S. Patent 4746348, 1962.

[29] C. Sharma and C. S. P. Ojha, "Statistical parameters of hydrometeorological variables: standard deviation, SNR, skewness and kurtosis," in Advances in Water Resources Engineering and Management: Select Proceedings of TRACE 2018, Springer Singapore, 2020.